PCCP

The Effect of Fluorophore Incorporation Method on Fluorescence Enhancement in Colloidal Photonic Crystals

Journal:	*Physical Chemistry Chemical Physics*
Manuscript ID	CP-ART-10-2015-006489.R1
Article Type:	Paper
Date Submitted by the Author:	17-Nov-2015
Complete List of Authors:	Eftekhari, Ehsan; Griffith University, Queensland Micro- and Nanotechnology Centre cole, ivan; CSIRO Materials Science and Engineering Li, Qin; Griffith University, Queensland Micro- and Nanotechnology Centre; Griffith University, Environmental Engineering

Journal Name

ARTICLE

The Effect of Fluorophore Incorporation Method on Fluorescence Enhancement in Colloidal Photonic Crystals

Received 00th January 20xx,
Accepted 00th January 20xx

DOI: 10.1039/x0xx00000x

www.rsc.org/

Ehsan Eftekhari,[a] Ivan S. Cole[b] and Qin Li[a*]

The significant effect of photonic crystals (PhC) on fluorophore emission has recently received intense interest. However, so far little attention has been paid on the influence of the fluorophore incorporation method on the performance of PhCs, particularly in practical applications. In this study, Rhodamine B is immobilised by a diffusion-swelling method on polystyrene spheres, which are self-assembled into three-dimensional colloidal photonic crystals films. This immobilization method has resulted in 230-fold fluorescence enhancement compared to control film, the greatest fluorescence enhancement of RhB immobilised on monolithic colloidal photonic crystals compared to other immobilization methods such as infiltration and electrostatic charge-facilitated dye attachment on particle surface. We further demonstrate the stability of dye attachment and the relationship between fluorescence intensity enhancement and the pseudo bandgap position relative to fluorophore fluorescence peak.

Introduction

Photonic crystals (PhCs) are artificial periodic structures consisting of different dielectric materials where the index of refraction varies on length scales of the wavelength of light. The periodic dielectrics contrast induces a forbidden region for electromagnetic waves, namely the photonic bandgap, or stopband for partial bandgap. The photonic bandgap and the 'slow photons' effect at the bandgap edges provides powerful means to control light.[1, 2] Self-assembled colloidal photonic crystals (CPhCs) from monodisperse colloidal particles, often polystyrene (PS) or silica spheres, offer an easily accessible and inexpensive platform for studying and device fabrication by manipulating photonic stopband.[3, 4]

CPhCs have shown strong effect on fluorescence (FL) emission.[5-10] Depending on the relative position between the FL emission maxima and stopband minima, the CPhCs can either inhibit or enhance emission.[1, 9-11] In the CPhCs, fluorescence can be enhanced by taking advantage of guided-mode resonances associated with enhanced extraction.[12] Enhanced extraction is the increasing of the emitted light resulting from coupling of fluorophore to leaky modes of CPhCs overlapping the emission wavelength.[5, 13] Song and co-workers reported 40-fold fluorescence enhancement by using monolithic CPhCs for optical storage,[14] and a 162-fold fluorescence enhancement by using heterostructure CPhCs.[15] 71-fold fluorescence enhancement was also observed by using CPhCs.[16]

CPhCs provide increased opportunities to control the fluorescence emission by overlapping photonic stopband with excitation and emission of the fluorophores. Although both excitation and emission wavelength can be enhanced by CPhCs, the mechanism of fluorescence enhancement inside the CPhCs structure is complex.

In all CPhCs based fluorescence enhancement studies, fluorescent dye was introduced into CPhCs architectures by infiltration,[17-19] or coating.[20, 21] However, the way the fluorescence dyes are introduced into the photonic crystals structure and its effect on the resulting fluorescence intensity have not been systematic investigated. This may have also made the quantitative comparisons among different studies unattainable. Therefore, establishing the relationship between dye position inside the CPhCs structures and fluorescence enhancement is important to help us understand better the effect of photonic crystal structures on fluorescence, as well as for developing the simple and highly efficient fluorescent CPhCs for different applications, particularly for sensing.

For many applications, it is highly desirable to develop a more robust, facile, stable and cost-effective approach to introduce dye into CPhCs structure, which is crucial for the integration of CPhCs into different applications. For instance, many applications such as sensing, coating and bioimaging are associated with liquid phase, it is important to stably immobilise the dye on the surface of the CPhCs porous structures.

[a] Queensland Micro- and Nanotechnology Centre, and Environmental Engineering, Griffith University, Nathan Campus, QLD 4111, Australia. E-mail: qin.li@griffith.edu.au; Tel: (61)(07)37357514
[b] CSIRO Materials Science and Engineering, Clayton, VIC 3168, Australia.

†Electronic Supplementary Information (ESI) available: The confocal images are presented in Fig. S1. The effect of DMF treatment time on fluorescence intensities is summarised in Fig. S2. More detailed results regarding the SEM images and normalised UV-vis transmissions are provided in Fig. S3-S4. For additional comparison details of coating see Fig. S5. See DOI: 10.1039/x0xx00000x

To address these demands, herein, we present a swelling-diffusion approach for a 'under the skin coating' of Rhodamine B (RhB) on PS colloids' surface. The stability of the immobilized dyes in photonic structure, and the effect on fluorescence intensity enhancement have been compared among three different immobilization approaches, namely 'under the skin coating' versus infiltration, and electrostatic charge-facilitated attachment (dubbed as 'superficial coating').

Experimental

Materials

Dimethyl formamide (DMF), tetrahydrofuran (THF), acrylic acid, acetone, ethanol and Rhodamine B (all purchased from Sigma Aldrich), were of analytical grade and used as received without further purification. Glass slides were used as the substrates for fabrication of CPhCs.

Synthesis and Fabrication

Polystyrene spheres (PS) with the size of 285 ±5 nm (small), 300 ±5 nm (medium) and 310 ±5 nm (large) were synthesized by an emulsifier free emulsion polymerisation method as per earlier report.[22] Acrylic Acid functionalised colloidal suspension, containing large spheres and carboxyl group on the surface were first synthesised and purified by several cycles of centrifugation. A 10^{-3} molL^{-1} solution of RhB was prepared in ethanol for its use as the model fluorescence dye.

To experimentally investigate the performance difference of the different dye-incorporation methods, namely infiltration, superficial coating and under-the-skin coating, three monolithic CPhC films were fabricated on the glass substrates by horizontal deposition method:[23]

1) Infiltration: self-assembly of 1 mL of acrylic acid functionalized large spheres (5 vol %) to form monolithic film followed by infiltrating 2 mL of RhB (10^{-2} molL^{-1}) dispersed in ethanol, the sample is denoted as RhB–infiltrated film.

2) Superficial Coating: mixing 1 mL of washed large acrylic acid functionalized PS suspension (5 vol %) with 2 mL of RhB (10^{-2} molL^{-1} in ethanol) for 24 hr. Due to the electrostatic charge interaction between carboxylic group on PS and amine group on RhB, binding between RhB and PS spheres occurs and the sample is denoted as RhB–large. Then RhB–large spheres were washed and purified by several cycles of centrifugation before being self-assembled into monolithic RhB–large film by horizontal deposition.

3) 'Under the skin' coating: RhB-immobilised small, medium and large spheres were obtained through diffusion and entrapment method and named as RhB@small, RhB@medium and RhB@large, respectively. [24] In detail, PS suspensions (5 vol %) were first purified by several cycles of centrifugation. 0.2 mL of RhB (10^{-2} molL^{-1} in ethanol) was mixed with 1.8 mL of DMF, resulting in 2 mL of RhB 10^{-3} molL^{-1} solution, which was added dropwise to 1 mL of washed large acrylic acid functionalized PS suspension. After a period of mixing ranging from 2 min up to 20 min, the RhB-coated PS spheres were washed and purified by several cycles of centrifugation. The monolithic CPhC films were fabricated on the glass substrates by self-ssembly of RhB@small, RhB@medium and RhB@large spheres by horizontal deposition method.[23] The reason that a lower RhB solution concentration of 10^{-3} molL^{-1} was used in this method in comparison to that in the former two methods (10^{-2} molL^{-1}), is because at 10^{-2} molL^{-1} concentration (in the solvent of ethanol mixed with DMF 1:9), the immobilised RhB already showed self-quenching effect owing to the higher dye loading efficiency of under-the-skin coating method. To illustrate this point, a concentration-dependence study has been performed; for all three dye incorporation methods, the concentration of RhB solution varied from 10^{-12} to 10^{-1} molL^{-1}, and the FL intensity of the resultant CPhC films were measured and compared.

To create the same chemical environment as the host of the dye molecules for FL intensity comparison, the reference sample is prepared as such: Large spheres were self-assembled by horizontal method on the glass then heated at 120 °C for 2 h to melt and form an amorphous film followed by drop casting 2 mL of RhB (10^{-2} molL^{-1}) in ethanol. This reference sample is referred to as a control film.

Stability Test

To experimentally prove the diffusion and penetration of RhB on PS surface, we designed the stability test. The four step solvent treatments were designed as follow: 1) RhB@large and RhB–large were separately mixed in DI water by ultrasonication for 5 mins. Centrifugation was then applied to separate the spheres and the solution, and the supernatant solution was collected for FL analysis. 2) RhB@large and RhB–large were separately mixed in 98% ethanol by ultrasonication for 5 mins. Centrifugation was then applied to separate the spheres and the solution, and the supernatant solution was collected for FL analysis. 3) The ethanol treated RhB@large and RhB–large spheres were separately mixed in 98% acetone by ultrasonication for 5 mins. Centrifugation was then applied to separate the spheres and the solution, and the supernatant solution was collected for FL analysis. 4) The ethanol/acetone treated RhB@large and RhB–large spheres were dispersed in 50% THF by ultrasonication for 5 mins, respectively. Supernatant solution and the spheres were separated by centrifugation. The supernatant from each step was checked by FL measurement to measure of leached RhB dyes from the coated spheres. The procedure for pH stability test was performed at the room temperature and consisting of: RhB@large and RhB–large films were immersed in acidic or basic solutions into the quartz cuvette. Each time, a 15 min time interval was given to allow a good diffusion-driven mixing in the cuvette, before the pH measurement.

Characterization

The surface morphology was examined by scanning electron microscope (SEM) using a JEOL 7001, operated at 15 kV. Transmission spectra were measured on an Agilent 8453 UV-Vis spectrometer. FT-IR spectra were collected on a Perkin-Elmer Spectrum 100 with a resolution of 4 cm^{-1} in transmission

mode. A baseline correction was applied after the measurement. Fluorescence emission spectra were recorded on a Thermo Scientific Lumina fluorescence spectrometer. All pH values were measured with a PH-4 INESA digital pH meter. An Olympus FV1000 confocal microscope using a green channel was used for the fluorescence microscope image of RhB@large using a x100 oil immersion objective.

Results and Discussion

As shown schematically in Fig. 1, the 'under-the-skin' coating of RhB on the PS spheres consists of three main processes: firstly, swelling of PS suspension by DMF; secondly, diffusion and penetration of RhB on the PS spheres and lastly, washing and removal of excess DMF. Monolithic CPhC films were then formed by self-assembly of dye-coated PS spheres. The swelling agent is important for identifying the suitable swelling medium to create sufficiently big pores on sphere surface without destroying the spheres. Previous reports have shown that DMF is a suitable swelling agent for polystyrene colloids,[25, 26] therefore RhB molecules are able to diffuse into the swelled skin layer of PS. By changing the DMF solvent back to water, the swelled PS polymer layer collapses and entraps the RhB molecules in the skin layer.

The dye-incorporation efficiency was indicated by fluorescence spectroscopy. The confocal microscopic images presented in Supporting Information (Figure S1) show that the RhB@large spheres are brightly red-emitting. However, the x100 objective cannot resolve the RhB distribution on sphere at the single molecule level. Figure S2 shows the evolution of fluorescence spectra of RhB@large, RhB@medium and RhB@small films with different DMF treatment time. The FL intensity for all three films increased with the increase in DMF treatment time (2 to 20 mins), suggesting as the longer exposure to DMF and RhB has allowed increased loading of RhB molecules in the skin layer of PS spheres. However, after 20 mins DMF treatment time, FL intensity decreased. This is likely due to higher swelling rate of PS spheres, which may have resulted in too large pores in the swelled layer, leading to reduced entrapment effect for 'locking in' the dye molecules.[26]

We examined the influence of DMF on PS by measuring the size of PS spheres by SEM. Table 1 shows the results for the effect of DMF on diameter size of PS spheres. With the same amount of optimised volume of DMF and exposure time for the PS suspensions of all three sizes, original size of PS spheres slightly increased by 10 nm. This can be understood as the swelling of PS spheres due to DMF treatment and penetration of RhB into PS matrix. The SEM images in Fig. 2 show the high ordering of the RhB-'under the skin' coated colloidal crystals film formed by self-assembly of RhB@large (Fig. 2(a)), RhB@small (Figure S3(a)) and RhB@medium (Figure S3(b)) spheres on glass, where large-area, high quality 3D monolithic fluorescent CPhC films are revealed. All three films exhibit face-centred cubic (FCC) crystal morphology with (1 1 1) planes oriented parallel to the surface of the substrate. The size selection of PS was based on the emission peak of RhB using Bragg's diffraction calculation:[27]

$$\lambda_{max} = 2d_{(111)}\sqrt{n_{eff}^2 - sin^2\theta} = 2\sqrt{\frac{2}{3}}.D.\sqrt{n_{eff}^2 - sin^2\theta} \quad (1)$$

Where λ_{max} indicates the wavelength value of the reflection peak, $d_{(111)}$ the distance between adjacent (111) lattice planes, D is the sphere diameter and n_{eff} is the effective refractive index of the structure, which is calculated by $n_{eff}^2 = \sum f_i n_i^2$, with n_i denoting the refractive index of the respective phase and f_i denoting the filling fraction of them. The small, medium and large spheres were synthesised with sphere sizes of 285, 300 and 310 nm, respectively (see Table. 1).

Figure 2(b) shows the transmission spectrum of large PS spheres monolithic film before (black line) and after under the skin coating (red line). It is observed that due to the slightly increased PS particle size which resulted in increased lattice constant after 'under the skin' coating process, the crystal appearance changed as the stop band red-shifted from 605 nm to 625 nm. The red-shift of the stopband peak position is also caused by the increased refractive index (n_{PS} ≈ 1.59, n_{RhB} = 1.65, n_{air} = 1) due to dye attachment. Stopband positions of RhB@small and RhB@medium were also red shifted to the longer wavelength, as shown in Figure S4 (a) and (b).

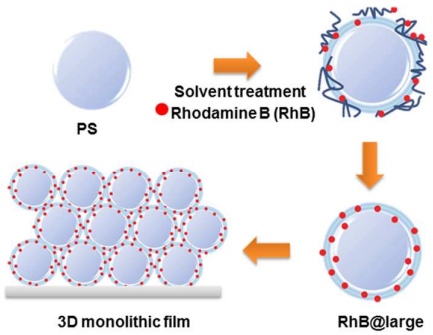

Fig. 1 Schematic of 3D monolithic RhB@large film fabrication, large PS suspension is treated with a solution of RhB in DMF resulting in entrapment of RhB on the surface of large PS spheres.

Table 1 Parameters of RhB under the skin coating PS spheres

	Sample	Sphere diameter (nm)	Calculated stopband (nm)	Experimental stopband (nm)
Before under skin coating	small	285	555	558
	medium	300	585	585
	large	310	604	605
After under skin coating	RhB@small	295	575	575
	RhB@medium	310	604	608
	RhB@large	320	623	625

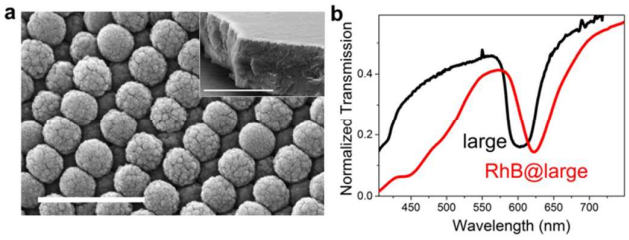

Fig. 2 (a) Top view SEM images of: RhB@large, scale bar is 1 µm. Inset: cross section SEM image of RhB@large film, scale bar is 10 µm. **(b)** Normalised UV-vis transmission before immobilisation (large) and after immobilisation with RhB (RhB@large).

Notably, the transmission peaks are still very sharp and highly symmetrical with almost unchanged FWHM (full width half maximum) for all three films, thereby implying the uniform immobilisation of RhB without any damage to the structural order of the CPhCs.

In this study, three different approaches were used to introduce RhB into the CPhCs structure: by infiltrating, superficial coating and 'under the skin' coating. In the superficial coating, RhB molecules are bonded to the surface of PS spheres through electrostatic charge interactions utilising the amine moiety of RhB and carboxylic group on PS surface, whilst in the 'under the skin' coating method, RhB molecules are primarily physically bound to PS surface mainly through the entanglement of the polymer chains. In order to examine the bonding mechanisms, the FTIR spectroscopy was performed and spectra of uncoated large PS spheres along with the RhB alone, RhB@large and RhB–large PS spheres are shown in Figure S5. For the carboxyl-group functionalised large PS, a broad shoulder between 3000 and 3700 cm^{-1} is attributed to the –OH stretching mode and the peak at 1640 cm^{-1} is assigned to the C=O stretching vibrations of carbonyl group, which indicate the presence of –COOH functional groups on large PS spheres.[28]

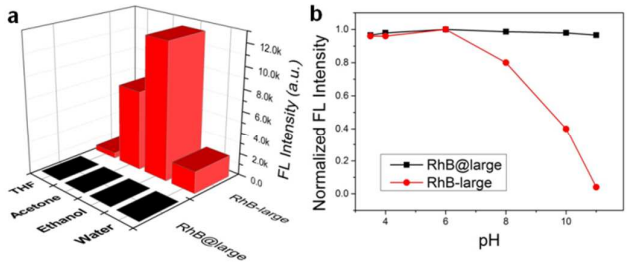

Fig. 3 (a) The fluorescence spectra of supernatant solutions of treated RhB@large and RhB-large with water, ethanol, acetone and THF. (b) The effect of pH on the fluorescence emission intensity of RhB@large and RhB-large.

Overall, the FTIR spectra show that both RhB@large and RhB–large modified PS spheres have successfully immobilized RhB molecules on PS spheres. The absence of new peaks in both systems confirms that both of these immobilization methods are based on physical interactions between RhB and PS surface.

To investigate the stability of RhB fixed on large PS surface in water or solvents, a stability test was designed for RhB@large compared to RhB–large spheres. Spheres were successively treated with water, ethanol, acetone and THF to demonstrate the difference in the stability of the 'under the skin'-coated RhB on the large PS spheres compared to electrostatic interaction-facilitated RhB coating. Figure 3(a) shows the FL intensity of supernatant solution (or washing solution) of RhB@large and RhB–large after treating with water, ethanol, acetone and THF.

In all four washing steps, the washing solutions for RhB–large all resulted in pink-coloured supernatants, indicating that some of the RhB dye leached out from the large PS spheres. In contrast, there was no detectable fluorescence signal from all four washing solutions of RhB@large, suggesting that RhB was strongly entrapped on the surface of RhB@large. The results confirm that the diffusion and penetration approach is very effective in immobilising RhB molecules on large PS surface.

Due to the poor stability in acidic and basic environment, most

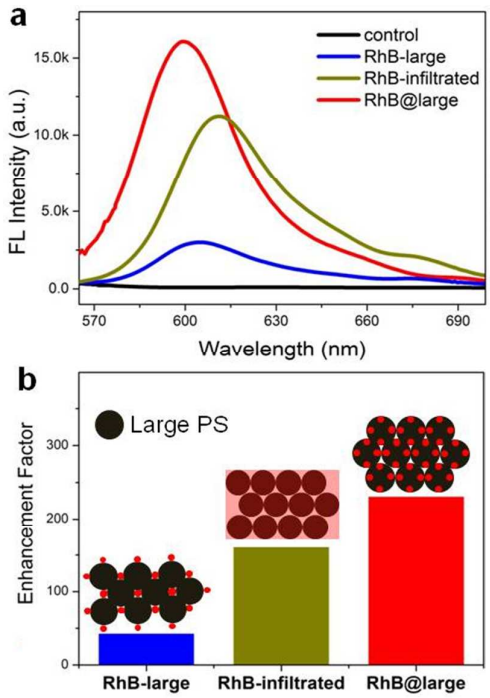

Fig. 4 (a) The fluorescence spectra of monolithic RhB@large, RhB-large, RhB-infiltrated and control films. **(b)** Enhancement factor for RhB@larg, RhB-large, RhB-infiltrated films compare to control film.

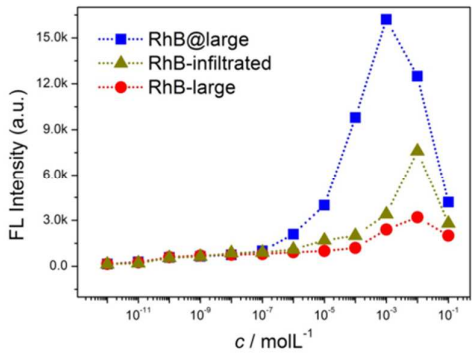

Fig. 5 Fluorescence intensities of CPhC films comprising of RhB@PS spheres prepared with 2ml of RhB at different concentrations (10^{-1} to 10^{-12} molL^{-1}) coated on large PS spheres by under-the-skin (RhB@large film) and superficial (RhB-large film) coating, and infiltrated in large PS film (RhB-infiltrated).

of previously reported fluorescence dye infiltrated in CPhCs shown pH-dependent response, which are likely caused by unstable dye corporation and limit their applications for physiological or environmental samples. Our newly designed fluorescent CPhCs is simple and more stable which should afford pH-independent response. Figure 3(b) shows the effects of pH on the fluorescence response of the RhB@large versus RhB–large. The experiments were carried out within a pH range from 3.5 to 11 for both films. As shown in Fig 3(b), the emission intensity of RhB@large did not vary with the pH value in a wide range from 3.5 to 11, suggesting that the response of our new fluorescent CPhC film is pH-independent; whilst the RhB-large CPhC film experienced drastic FL drop after being immersed in aqueous solutions of pH > 6. This significant contrast is because that the electrostatic interaction between –COOH group on PS spheres and -NH_2 moiety on RhB requires hydrogen bonding to facilitate, which is sensitive to pH, however the 'under the skin' method is utilising polymer chain entanglement, therefore pH independent. Such a stable fluorescent CPhCs film in a wide pH range is desirable for practical applications in complex biological or environmental samples, as there is no need to adjust the pH value of the sample.

The fluorescence spectra of RhB@large, RhB–large and RhB-infiltrated films and the enhancement factors measured relative to the control film excited by 460 nm are displayed in Fig. 4 (a) and (b). All films show significant enhancement of fluorescence intensity of RhB compared to the control film. It is also apparent that the method of incorporation of RhB on large PS spheres has a considerable impact on the magnitude of enhancement. Spectral reshaping of fluorescence is likely due to the slight change in PS sphere diameter during the DMF treatment (as mentioned before) as well as the mean refractive index differences induced by the different dye-incorporation methods. As illustrated by Equation (1), both changes would lead to shifts in the pseudo bandgap position of the CPhC films that are coupled with the fluorescent emission.[29]

We have observed that the incorporation of dye into the CPhCs structure had significant impact on the fluorescence enhancement. As shown in Fig. 4(b) the RhB@large film exhibited a significantly high fluorescence enhancement factor of 230-fold compared to RhB-infiltrated film of 160-fold and RhB–large film of 40-fold. The fluorescence enhancement is owing to the fact that the stopband overlaps the emission of RhB which can serve as the dielectric cavity and act as a local resonance mode for the emission propagation.[30, 31] The difference in enhancement magnitude between RhB@large and RhB–large films can be attributed to the higher efficiency in RhB loading with the 'under the skin' coating method. The difference in enhancement magnitude between RhB@large and RhB-infiltrated is more intriguing, because quantity-wise the RhB dye loading should be the highest in RhB-infiltrated method. Two factors may have contributed to this effect: a.) infiltration of RhB molecules in the interstitial volume of the CPhC film may result in localized agglomeration of dye molecules, which reduces FL intensity due to self-quenching.[32, 33] In contrast, the 'under the skin' coating method results in homogenous distribution of RhB dyes over the PS spheres; b.) 'under the skin' coating results in confinement of emissive species in solid phase of the CPhC film, whilst the infiltration

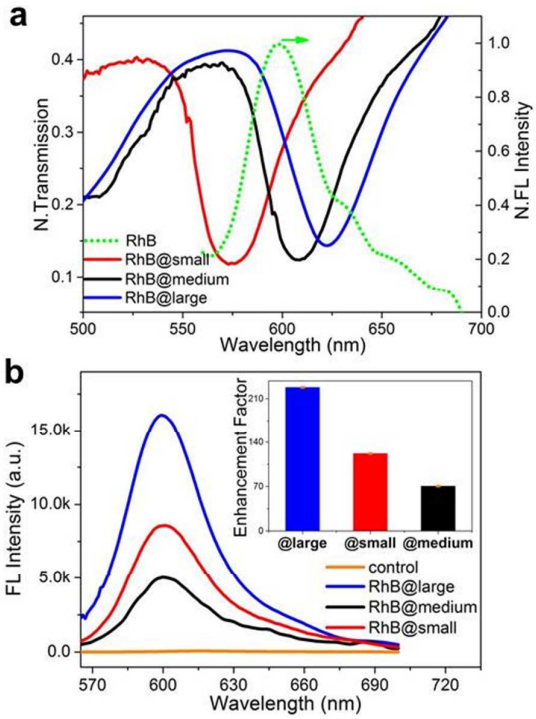

Fig. 6 (a) The normalise transmission spectra of monolithic RhB@large, RhB@medium and RhB@small films overlaid with the normalized fluorescence emission spectra of RhB. **(b)** The fluorescence spectra of monolithic RhB@large, RhB@medium and RhB@small films and control film. Inset: enhancement factor for RhB@large, RhB@medium and RhB@small films compare to control film.

method may lead to accumulation of dye molecule in the interstitial void of the CPhC structure, which reduces the refractive index contrast of the periodic structure, therefore reducing the photonic effect. It is also worth noting that on RhB-infiltrated FL spectra, there is a small peak around 680 nm, which is absent in both RhB@large and RhB-large. As discussed in,[34] this small FL peak is due to the RhB molecules that are accumulated on the top surface of the CPhC film.

To further demonstrate the better enhancement performance of the RhB@large film, we systematically compared the fluorescence intensities with RhB–infiltrated and RhB–large films at different concentrations of RhB from 10^{-1} to 10^{-12} molL^{-1} (in preparation solution). Figure 5 shows fluorescence intensities of RhB in CPhC films with the three different dye-loading methods at different concentrations. The results showed that the RhB@large film reached the highest FL signal at the concentration of 10^{-3} molL^{-1} while RhB–infiltrated and RhB–large films reached the highest FL signal at the higher concentration of 10^{-2} molL^{-1}, and the highest intensity of RhB@large film is more than two-fold stronger than that of RhB-infiltrated. The following decline of FL when dye concentration further increases in all three systems is due to dye self-quenching.[32, 33] The result confirms that the better dye-loading efficiency with the 'under the skin' coating method.

Since the 'under the skin' coating method offers better control on the location of dyes in CPhC films, it provides a better defined system to study the effect of photonic crystal structure on fluorophore emissions. Figure 6(a) shows the stopbands of RhB@large, RhB@medium and RhB@small films and their relative positions with reference to the emission of RhB. As shown in Fig. 6(a), FL emission of RhB overlapped the red edge, slightly-off-stopband and blue edge of photonic stopband of RhB@small, RhB@medium and RhB@large films, respectively.

The effect of the relative position between the photonic stopband and the dye emission maximum on the FL intensity is presented in Fig. 6(b). The emission of RhB was enhanced at the edges of the stop band, especially at the blue edge, so the RhB@large with stop band at 625 nm experienced stronger enhancement compared to RhB@small with stop band at 575 nm. It is observed that the FL signal is enhanced at the band edge and suppressed inside the stopband.[35-38]

The 230-fold enhancement is due to the overlap of emission light with the blue edge of stopband of RhB@large film. A 120-fold enhancement was achieved when the emission light overlapped the red edge of stopband of RhB@small film while only a 70-fold enhancement was observed when the emission light is slightly off the stopband of RhB@medium film. The FL enhancement behaviour observed here is consistent with former reports that when the fluorophore emission peak overlaps the blue or red edge of photonic band gap, the emission light intensity enhances.[4, 39]

Conclusion

In this study, we demonstrated that diffusion-swelling method is a highly effective method for immobilising fluorophores, [24] such as Rhodamine B on polystyrene spheres, which can then self-assembled into colloidal photonic crystals films. This diffusion-swelling dye coating method utilises polymer swelling and deswelling behaviour and achieved stable 'under the skin' coating without resorting to covalent bonding. Compared to the electrostatic charge facilitated coating, 'under the skin' coating shows higher dye loading efficiency, excellent stability in wide pH range (3.5 – 11) and minimum leaching effect in water and various solvents.

Moreover, when assembled into CPhCs, by matching the RhB emission peak with the CPhC stop band blue edge, the RhB coated CPhC film has exhibited 230-fold fluorescence enhancement, significantly higher than the performance of CPhC films that incorporated the dyes by electrostatic charge interactions or infiltration when the same quantity of dyes were applied during fabrication. The better performance can be attributed to higher efficiency in dye loading and the homogeneous distribution of dye molecules within the CPhC structure.

Such a homogeneous and stable fluorophore incorporation method would allow us to better control the dye location in PhC structures, enhance enable in-depth studies of PhC influence on emissions. Furthermore, such a robust and stable fluorophore coating method will allow practical applications of such a FL enhancement platform, for example in chemical and biochemical sensing.

Acknowledgements

Ehsan Eftekhari acknowledges the support of a Griffith University International Postgraduate Research Scholarship and a CSIRO OCE top-up scholarship. Qin Li acknowledges the support of a Griffith University Research Infrastructure Grant and School of Engineering Strategic Funding. The authors appreciate the access to the electron microscopes at the Centre for Microscopy and Microanalysis at the University of Queensland and wish to thank Ms Maria Nguyen at the Eskitis Institute, Griffith University for performing the confocal microscopy analysis.

References

1. E. Yablonovitch, *Physical Review Letters*, 1987, **58**, 2059-2062.
2. S. John, *Physical Review Letters*, 1987, **58**, 2486-2489.
3. X. Cui, K. Tawa, K. Kintaka and J. Nishii, *Advanced Functional Materials*, 2010, **20**, 945-950.
4. H. Li, J. Wang, Z. Pan, L. Cui, L. Xu, R. Wang, Y. Song and L. Jiang, *Journal of Materials Chemistry*, 2011, **21**, 1730-1735.
5. N. Ganesh, I. D. Block, P. C. Mathias, W. Zhang, E. Chow, V. Malyarchuk and B. T. Cunningham, *Optics Express*, 2008, **16**, 21626-21640.
6. A. Pokhriyal, M. Lu, V. Chaudhery, C.-S. Huang, S. Schulz and B. T. Cunningham, *Optics Express*, 2010, **18**, 24793-24808.

7. A. Pokhriyal, M. Lu, C. Ge and B. T. Cunningham, *Journal of Biophotonics*, 2014, **7**, 332-340.
8. R. Badugu, K. Nowaczyk, E. Descrovi and J. R. Lakowicz, *Analytical Biochemistry*, 2013, **442**, 83-96.
9. L. Bechger, P. Lodahl and W. L. Vos, *Journal of Physical Chemistry B*, 2005, **109**, 9980-9988.
10. P. V. Braun, S. A. Rinne and F. Garcia-Santamaria, *Advanced Materials*, 2006, **18**, 2665-2678.
11. C. Vion, C. Barthou, P. Benalloul, C. Schwob, L. Coolen, A. Gruzintev, G. Emel'chenko, V. Masalov, J.-M. Frigerio and A. Maitre, *Journal of Applied Physics*, 2009, **105**.
12. V. Chaudhery, S. George, M. Lu, A. Pokhriyal and B. T. Cunningham, *Sensors*, 2013, **13**, 5561-5584.
13. N. Ganesh, W. Zhang, P. C. Mathias, E. Chow, J. A. N. T. Soares, V. Malyarchuk, A. D. Smith and B. T. Cunningham, *Nature Nanotechnology*, 2007, **2**, 515-520.
14. H. Li, J. Wang, H. Lin, L. Xu, W. Xu, R. Wang, Y. Song and D. Zhu, *Advanced Materials*, 2010, **22**, 1237-1241.
15. H. Li, J. Wang, F. Liu, Y. Song and R. Wang, *Journal of Colloid and Interface Science*, 2011, **356**, 63-68.
16. C.-a. Tao, W. Zhu, Q. An, H. Yang, W. Li, C. Lin, F. Yang and G. Li, *J. Phys. Chem. C*, 2011, **115**, 20053-20060.
17. G. R. Maskaly, M. A. Petruska, J. Nanda, I. V. Bezel, R. D. Schaller, H. Htoon, J. M. Pietryga and V. I. Klimov, *Advanced Materials*, 2006, **18**, 343-+.
18. T. Akimoto and M. Yasuda, *Applied Optics*, 2010, **49**, 80-85.
19. W. Zhang and B. T. Cunningham, *Applied Physics Letters*, 2008, **93**.
20. J. Feng, S. Yang, D. Xian-Zi, C. Wei-Qiang and D. Xuan-Ming, *Applied Physics Letters*, 2007, **91**, 031109-031101-031103.
21. Z.-q. Liu, G.-q. Liu, Y.-h. Chen, K. Huang, X.-n. Zhang, Z.-j. Cai and Y. Hu, *Optics Communications*, 2013, **301–302**, 34-38.
22. P. H. Wang and C. Y. Pan, *Colloid and Polymer Science*, 2002, **280**, 152-159.
23. Z. Zhou, Q. Yan, Q. Li and X. S. Zhao, *Langmuir*, 2007, **23**, 1473-1477.
24. J.-H. Lee, I. J. Gomez, V. B. Sitterle and J. C. Meredith, *Journal of Colloid and Interface Science*, 2011, **363**, 137-144.
25. L. K. Wang, Y. Wan, Y. Q. Li, Z. Y. Cai, H. L. Li, X. S. Zhao and Q. Li, *Langmuir*, 2009, **25**, 6753-6759.
26. V. K. Sarin, S. B. H. Kent and R. B. Merrifield, *J. Am. Chem. Soc.*, 1980, **102**, 5463-5470.
27. S. E. Shim, Y. J. Cha, J. M. Byun and S. Choe, *Journal of Applied Polymer Science*, 1999, **71**, 2259-2269.
28. W. L. Zhang, Y. D. Liu and H. J. Choi, *Journal of Materials Chemistry*, 2011, **21**, 6916-6921.
29. B. Y. Ding, C. Hrelescu, N. Arnold, G. Isic and T. A. Klar, *Nano Letters*, 2013, **13**, 378-386.
30. A. C. Arsenault, D. P. Puzzo, I. Manners and G. A. Ozin, *Nature Photonics*, 2007, **1**, 468-472.
31. J. I. L. Chen, G. von Freymann, S. Y. Choi, V. Kitaev and G. A. Ozin, *Advanced Materials*, 2006, **18**, 1915-+.
32. J. Hou, H. C. Zhang, Q. Yang, M. Z. Li, Y. L. Song and L. Jiang, *Angewandte Chemie-International Edition*, 2014, **53**, 5791-5795.
33. X. Wang, S. Xu and W. Xu, *Physical Chemistry Chemical Physics*, 2011, **13**, 1560-1567.
34. E. Eftekhari, X. Li, T. H. Kim, Z. Gan, I. S. Cole, D. Zhao, D. Kielpinski, M. Gu and Q. Li, *Scientific Reports*, 2015, **5**, 14439.
35. C. Blum, A. P. Mosk, I. S. Nikolaev, V. Subramaniam and W. L. Vos, *Small*, 2008, **4**, 492-496.
36. A. G. Galstyan, M. E. Raikh and Z. V. Vardeny, *Physical Review B*, 2000, **62**, 1780-1786.
37. P. Lodahl, A. Floris van Driel, I. S. Nikolaev, A. Irman, K. Overgaag, D. Vanmaekelbergh and W. L. Vos, *Nature*, 2004, **430**, 654-657.
38. M. Megens, J. E. G. J. Wijnhoven, A. Lagendijk and W. L. Vos, *J. Opt. Soc. Am. B*, 1999, **16**, 1403-1408.
39. M. Li, F. He, Q. Liao, J. Liu, L. Xu, L. Jiang, Y. Song, S. Wang and D. Zhu, *Angewandte Chemie International Edition*, 2008, **47**, 7258-7262.